Alkyltin Keggin clusters as EUVL photoresist technology

Rebecca D. Stern, Danielle C. Hutchison, Morgan R. Olsen, Lev N. Zakharov, May Nyman, et al.

Rebecca D. Stern, Danielle C. Hutchison, Morgan R. Olsen, Lev N. Zakharov, May Nyman, Kristin A. Persson, "Alkyltin Keggin clusters as EUVL photoresist technology," Proc. SPIE 11147, International Conference on Extreme Ultraviolet Lithography 2019, 111471L (26 September 2019); doi: 10.1117/12.2538639

SPIE.

Event: SPIE Photomask Technology + EUV Lithography, 2019, Monterey, California, United States

Alkyltin Keggin clusters as EUVL photoresist technology

Rebecca D. Stern*[a], Danielle C. Hutchison[b], Morgan R. Olsen[b], Lev N. Zakharov[c], May Nyman[b], Kristin A. Persson[a,d]

[a]Department of Materials Science and Engineering, University of California Berkeley, Berkeley, CA, 94720, USA *Email: rebecca.stern@berkeley.edu
[b]Department of Chemistry, Oregon State University, Corvallis, OR, 97331, USA
[c]Department of Chemistry and Biochemistry, University of Oregon, Eugene, OR, 97403, USA
[d]Lawrence Berkeley National Laboratory, Berkeley, CA, 94720, USA

ABSTRACT

Extreme ultraviolet lithography is the newest technique to keep up with Moore's law and create smaller integrated circuit feature sizes. However, novel photoresist materials must be used in order to withstand the high energy beam (λ=13.5nm). Metal-oxo clusters have been proposed as one photoresist solution, and specifically the most promising is a sodium-centered tin-Keggin cluster. A simple one-step synthesis was developed to produce a Na-Sn Keggin cluster, without the need for heating, filtration, or recrystallization. However, the product was a mixture of the β-isomer (β-$NaSn_{12}$) and the γ-isomer (γ-$NaSn_{12}$), which share the formula $[(MeSn)_{12}(NaO_4)(OCH_3)_{12}(O)_4(OH)_8]^{1+}$. For fundamental studies on the lithographic mechanisms occurring during exposure to be successful, a pure and stable isomer is desired. Computational modeling was recruited to determine the ground state energy of all five uncapped isomers in this Na-Sn Keggin system. Additionally, the inclusion of one or two tin atoms to the uncapped structure, called capping, altered which isomers were stabilized. Computations were also employed to evaluate the influence of this capping strategy for the single-capped β-isomer (β-$NaSn_{13}$), the single-capped α-isomer (α-$NaSn_{13}$), the single-capped γ-isomer (γ-$NaSn_{13}$), and the double-capped γ-isomer (γ-$NaSn_{14}$). Density functional theory (DFT) was used to obtain the hydrolysis Gibbs free energy and HOMO-LUMO gap, which led to the stability ranking: β-$NaSn_{12}$ > γ-$NaSn_{12}$ > α-$NaSn_{12}$ > δ-$NaSn_{12}$ > ε-$NaSn_{12}$ for uncapped clusters, which was consistent which experimental observations. The uncapped isomers were computationally evaluated to be more stable than their respective single-capped analogues. However, the double-capped γ-$NaSn_{14}$ was more stable than either the uncapped or single-capped clusters. Therefore, capping has shown to be a useful tool in exploring the stability landscape of these Keggin clusters to promote a pure and stable material for the next generation EUV lithography photoresists. And noteworthy, this sodium-centered tin-Keggin ion represents the only Keggin ion family so far, that favors the isomers of lower symmetry.

Keywords: Tin-oxo clusters, extreme ultraviolet lithography, Keggin, metal-oxo photoresists, computational, density functional theory, isomerization, hydrolysis Gibbs free energy

1. INTRODUCTION

With integrated circuit manufacturers aiming to produce sub-10nm feature sizes, extreme ultraviolet lithography (EUVL) is perceived as the next developing technology, at a wavelength of only 13.5nm.[1] The challenges with using polymer-based photoresists for EUVL can be eliminated by using metal-oxo cluster photoresists. Metal-oxo clusters are smaller than the bulky carbon chains in the polymer-based resists, thus preventing pattern collapse. Also, metal-oxo clusters are more durable during the lithographic etching step. Metal-oxo systems previously investigated as potential photoresist materials include hafnium, antimony, and tin clusters.[2–6] These systems have a high EUV atomic absorption cross-section, needed for proper resist functionality.[7] Each system had their limitations however. Hafnium-based clusters demonstrated 8nm resolution but resulted in background condensation.[2] Antimony-oxo clusters had EUV sensitivity but pattern collapse limited high resolution.[3] The tin-oxo "football" cluster prevented background condensation, but the synthesis was difficult.[4] A capped sodium-centered organotin-oxo Keggin cluster produced high aspect ratio and dense line patterns with helium ion beam lithography, but synthesis of the structure was difficult leading to poor reproducibility and low yields.[5,6]

International Conference on Extreme Ultraviolet Lithography 2019, edited by Toshiro Itani, Paolo A. Gargini, Patrick P. Naulleau, Kurt G. Ronse, Proc. of SPIE Vol. 11147, 111471L
 · doi: 10.1117/12.2538639

It is thought that the cleavage of the Sn-C bond of the terminal butyl ligands in this material is the cause of the change in the solubility of this photoresist.[8] In order to evaluate this system in more depth, a simplified synthesis strategy was required to further investigate the possibilities of a sodium center organotin-oxo Keggin cluster as a photoresist for EUV lithography.

Hutchison and coworkers recently discovered a simple one-step synthesis for the Na-Sn Keggin system that proceeds at room temperature and does not require any filtration or recrystallization.[9] This synthesis strategy successfully made the $[(MeSn)_{12}(NaO_4)(OCH_3)_{12}(O)_4(OH)_8]^{1+}$, which is an uncapped Keggin cluster denoted β-$NaSn_{12}$. However, this synthesis led to a mixture of uncapped β-$NaSn_{12}$ and uncapped γ-$NaSn_{12}$ isomers. Computational studies were recruited to investigate this dilemma and unknown cause. Since the Keggin geometry has 5 possible isomers, all 5 uncapped $NaSn_{12}$ isomers α, β, γ, δ, and ε, were computationally modeled in this paper. To evaluate the influence of capping on the prevention of isomerization between uncapped β-$NaSn_{12}$ and uncapped γ-$NaSn_{12}$, the experimentally observed capped β-$NaSn_{13}$ and γ-$NaSn_{13}$, as well as the most recently synthesized double capped γ-$NaSn_{14}$ were computationally modeled in this paper as well.[9,10] The advantages of using computational modeling tools is to be able to evaluate the thermodynamic stability of experimental as well as theoretical isomers of a given system. The calculated thermodynamic landscape of the isomers enables comparison of the isomer stability and hence interpretation of experimental results. Ideally, computational results will guide synthesis design, being able to determine the influential factors that drive stability between isomers and predict new structures.

2. DESCRIPTION OF STRUCTURES

2.1 The Keggin geometry

The Keggin cluster was first structurally characterized in 1934 by J.F. Keggin.[11] It contains a heteroatom metal center in a 4-coordinate environment. Surrounding this are four trimer units. Each trimer unit consists of three metals in a 6-coordinate environment. The three octahedra are edge-sharing within the trimer unit. The α-isomer is defined as having its four trimer units connected by corner-sharing between trimers, resulting in T_d symmetry, as shown in Figure 1. If one trimer unit is rotated by 60 degrees, the β-isomer is obtained which still exhibits only corner-sharing trimers but with a reduced symmetry of C_{3v}. Continuing this process of successive trimer rotations of 60 degrees, the γ-isomer of C_{2v} symmetry is obtained. Finally, a rotation of a third trimer yields the δ-isomer and a fourth trimer rotation yields the ε-isomer, possessing C_{3v} and T_d symmetries, respectively.

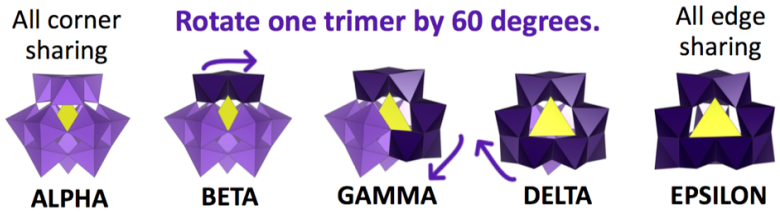

Figure 1. Trimer rotation to obtain five Keggin isomers α, β, γ, δ, and ε.

2.2 Situation I: Mixed β/γ-$NaSn_{12}$

The one-step synthesis strategy developed by Hutchison *et al.* occurred at room temperature and did not require any filtration or recrystallization.[9] However, ^{119}Sn-NMR and single-crystal x-ray diffraction showed a mixture of β-$NaSn_{12}$ and γ-$NaSn_{12}$. To investigate the isomerization, all five uncapped Na-Sn Keggin isomers (α, β, γ, δ, ε) were computationally modeled. They all were given the same formula: $[(MeSn)_{12}(NaO_4)(OCH_3)_{12}(O)_4(OH)_8]^{1+}$. The β-$NaSn_{12}$ and γ-$NaSn_{12}$ clusters are shown in Figure 2a and 2b, respectively. To decrease the computational cost and complexity of these models, the butyl Sn-terminal ligands were replaced with methyl ligands, a common practice.[12] In this Na-Sn Keggin system, the central heteroatom is sodium. Each trimer unit of the Keggin is comprised of three $MeSnO_5$ octahedra with a methyl terminal ligand on each tin atom. The three bridging oxygens within each trimer unit (12 total O^{2-}) are methoxy ligands. The bridging oxygens between the four trimer units (12 total O^{2-}) are oxo or hydroxyl ligands. The overall charge of the structures is determined by the total number of hydroxyl ligands. The location of the hydroxyl ligands impacts the hydrolysis Gibbs free energy and care was taken to obtain the lowest energy conformation. Although the hydrogen location

cannot be inferred from the x-ray diffraction data, mass spectrometry identified the overall charge of the structures and bond-valence sum helped guide the hydroxyl ligand placement.

2.3 Situation II: Single-capped β-$NaSn_{13}$

Saha *et al.* in 2017 produced a single-capped β-$NaSn_{13}$.[5] However, authors found impurities of uncapped $NaSn_{12}$ isomers and Sn_{12} (i.e. the 'football' cluster $[(RSn)_{12}O_{14}(OH)_6]^{2+}$, R=alkyl) co-crystallized with β-$NaSn_{13}$ in unknown quantities, as determined with electrospray ionization mass spectroscopy (ESI-MS) and ^{119}Sn-NMR. The computationally modeled β-$NaSn_{13}$ was assigned a formula of $[(MeSn)_{12}(NaO_4)(OCH_3)_{12}(O)_8(OH)_4(Sn(H_2O)_2)]^{1+}$ which is exactly consistent with the experimental crystal structure determined by ESI-MS.[9] The cap position and bonding for theoretical α-$NaSn_{13}$ was modeled after β-$NaSn_{13}$ since these two isomers exhibit similar symmetries and capping "windows" as compared to γ-$NaSn_{13}$. The cap on β-$NaSn_{13}$ and α-$NaSn_{13}$ is a 6-coordinate tin, with four bonds to the cluster in the tetragonal window. The two terminal ligands are waters. The single-capped β-$NaSn_{13}$ is shown in Figure 2c.

2.4 Situation III: Single-capped γ-$NaSn_{13}$

A different synthesis strategy conducted by Hutchison *et al*. produced single-capped γ-$NaSn_{13}$.[9] However, crystals of both γ-$NaSn_{13}$ and uncapped β-$NaSn_{12}$ were isolated from the same closed vial.[9] This computational study modeled the γ-$NaSn_{13}$ as $[(MeSn)_{12}(NaO_4)(OCH_3)_{12}(O)_6(OH)_6(Sn(Me)(OCH_3))]^{1+}$ as shown in Figure 2d. The cap is a 5-coordinate tin, with three bonds to the cluster in one of the pentagonal windows adjacent to the edge sharing trimer units. The two terminal ligands are methyl and methoxy.

2.5 Situation IV: Double-capped γ-$NaSn_{14}$

Zhu *et al.* very recently synthesized the double-capped γ-$NaSn_{14}$ in 2019.[10] This synthesis strategy successfully prevented isomerization, yielding pure γ-$NaSn_{14}$. Two 5-coordinate tin caps are found on the structure, one in each pentagonal window on either side of the edge shared between two trimer units. The terminal ligands are a butyl chain (modeled as methyl) and an oxygen atom from a $BO_2(OH)$ ligand. The two borate ligands provide a bridge between the tin cap and they each replace one methoxy ligand within a trimer unit. The authors believe the borate group stabilizes the cap, which in turn stabilizes the Keggin cluster. This structure is shown in Figure 2e.

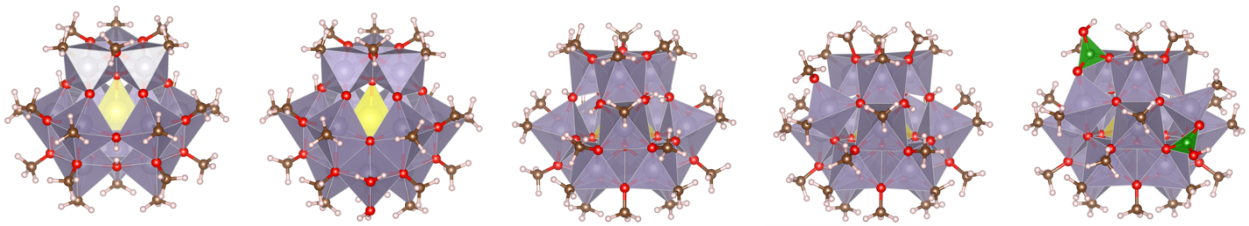

(a) (b) (c) (d) (e)

Figure 2. (a) uncapped β-$NaSn_{12}$, (b) single-capped β-$NaSn_{13}$, (c) uncapped γ-$NaSn_{12}$, (d) single-capped γ-$NaSn_{13}$, (e) double-capped γ-$NaSn_{14}$. Tin are purple octahedra, sodium is central yellow tetrahedra, carbon are brown, hydrogen are white, and boron are green.

3. METHODOLOGY

3.1 Approach

The experimentally isolated clusters were computationally modeled. These consisted of the two uncapped isomers (β-$NaSn_{12}$, γ-$NaSn_{12}$), the two single-capped isomers (β-$NaSn_{13}$, γ-$NaSn_{13}$), and the one double-capped isomer (γ-$NaSn_{14}$). Additionally, theoretical clusters (which have never been experimentally isolated) of the Na-Sn system were also modeled. These included three uncapped isomers (α-$NaSn_{12}$, δ-$NaSn_{12}$, ε-$NaSn_{12}$), and one single-capped isomer (α-$NaSn_{13}$), bringing the total number of systems investigated to nine.

We determined the hydrolysis Gibbs free energy (ΔG_{aq}) in solution by using a thermodynamic cycle in which the hydrolysis energy is the sum of the corresponding gas-phase Gibbs free energy (ΔG_{gas}) and the Gibbs free energies of solvation ΔG_{solv} as seen in Equation 1. The thermodynamic cycle is used to reduce errors when calculating the solvation energy and comparing structures of different formula.[13–16] The gas-phase Gibbs free energy contains a correction term that takes into account the enthalpy, entropy, and temperature of the system when a frequency analysis is conducted. The term "n" is the coefficient of that species. An example of this thermodynamic cycle using β-$NaSn_{12}$ is shown in Scheme 1. The dielectric constant for the solvent model was set to ~78.36, consistent with water.

$$\Delta G_{aq} = \Delta G_{gas} + \sum_{i=1}^{Nproducts} n_i \Delta G_i^{solv} - \sum_{j=1}^{Nreactants} n_j \Delta G_j^{solv} \quad (1)$$

Scheme 2. Thermodynamic cycle for β-$NaSn_{12}$.

$$12\,Sn(H_2O)_6{}^{4+}{}_{(aq)} + 6\,Na(H_2O)_6{}^{+}{}_{(aq)} + 3\,CO_{2(aq)} + 21\,CH_{4(aq)} \xrightarrow{\Delta G_{aq}} 48\,H_3O^+_{(aq)} + 8\,H_2O_{(aq)} + C_{24}H_{80}NaO_{28}Sn_{12}{}^{+}{}_{(aq)}$$

$$\downarrow -\Delta G^{solv}_{Sn(H_2O)_6^{4+}} \quad \downarrow -\Delta G^{solv}_{Na(H_2O)_6^{+}} \quad \downarrow -\Delta G^{solv}_{CO_2} \quad \downarrow -\Delta G^{solv}_{CH_4} \qquad \uparrow \Delta G^{solv}_{H_3O^+} \quad \uparrow \Delta G^{solv}_{H_2O} \quad \uparrow \Delta G^{solv}_{C_{24}H_{80}NaO_{28}Sn_{12}^+}$$

$$12\,Sn(H_2O)_6{}^{4+}{}_{(g)} + 6\,Na(H_2O)_6{}^{+}{}_{(g)} + 3\,CO_{2(g)} + 21\,CH_{4(g)} \xrightarrow{\Delta G_{gas}} 48\,H_3O^+_{(g)} + 8\,H_2O_{(g)} + C_{24}H_{80}NaO_{28}Sn_{12}{}^{+}{}_{(g)}$$

3.2 Computational details

The geometry of each cluster was first optimized using Gaussian 09 in the gas phase using the B3LYP functional.[17] The basis set 6-31G(d) was used for elements Na, Ca, C, H, and O, while the basis set LANL2DZ was used for the element Sn.[18,19] A subsequent frequency calculation was performed to verify the absence of imaginary vibration modes to confirm that the system is in a stable/metastable state. An effective core potential LANL2DZ was used for Sn. The geometry was further optimized in water using the continuum solvation model SMD.[20] The electronic energy was refined using a B3LYP single point with the basis set 6-311+G(d,p) for elements Na, Ca, C, H, and O, and basis set LANL2DZ for Sn.[21] The solvation energy was computed using a B3LYP/6-31G(d) single point with SMD for water (ε≈78.36).

4. RESULTS AND DISCUSSION

The hydrolysis Gibbs free energy in kcal mol^{-1} and HOMO-LUMO gap in eV are listed in Table 1 for each of the nine clusters investigated. The more stable clusters should exhibit a relatively low hydrolysis Gibbs free energy and a relatively large HOMO-LUMO gap. In our case, the stability ordering is evaluated by the hydrolysis Gibbs free energy. The HOMO-LUMO gaps are too close in energy to conclusively determine the isomer stability ordering, but rather used to support the results from the Gibbs free energy.

Table 1. Hydrolysis Gibbs free energy (kcal mol^{-1}) and HOMO-LUMO gap (eV) of uncapped and capped Na-Sn clusters.

Cluster	Hydrolysis Gibbs Free Energy (kcal mol^{-1})	HOMO-LUMO gap (eV)
ε-$NaSn_{12}^{1+}$	386.6	5.87
α-$NaSn_{13}^{1+}$	369.7	5.17
β-$NaSn_{13}^{1+}$	364.9	5.28
γ-$NaSn_{13}^{1+}$	361.2	5.80
δ-$NaSn_{12}^{1+}$	347.3	6.09
α-$NaSn_{12}^{1+}$	342.7	6.20
γ-$NaSn_{12}^{1+}$	337.4	5.91

β-$NaSn_{12}^{1+}$	327.4	6.24
γ-$NaSn_{14}$	272.3	6.04

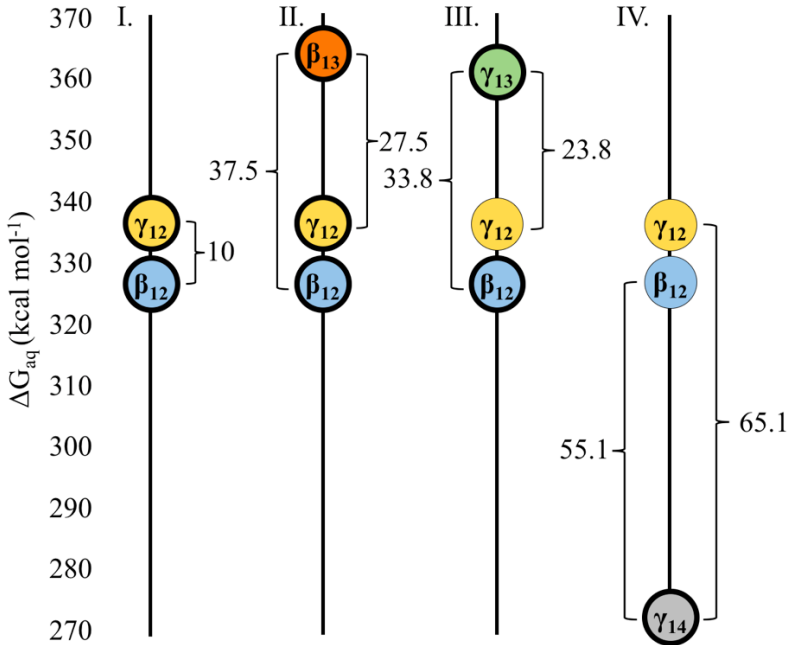

Figure 3. Four synthesis strategies (I, II, III, IV) and their experimentally observed results (bold-circled isomers). Hydrolysis Gibbs free energies of all relevant isomers are included. Blue = β-$NaSn_{12}$, Yellow = γ-$NaSn_{12}$, Red = β-$NaSn_{13}$, Green = γ-$NaSn_{13}$, Gray = γ-$NaSn_{14}$.

The uniqueness of the tin-oxo Keggin system is that it prefers the less symmetric isomers, β and γ. To our knowledge, no other Keggin cluster systems have been discovered where the β and γ isomers are the most stable. Traditional polyoxometalates like the W- and Mo-Keggin clusters prefer the α and β isomers.[22] The Al-Keggin and Sb-Keggin favor the ε isomer.[12,23] And the Cr-Keggin has been recently synthesized as the δ-isomer.[24,25] A visual guide for the joint results of the four synthesis strategies (bolded values) and the relevant isomer energy differences are shown in Figure 3. The hydrolysis Gibbs free energy differences between the uncapped clusters are similar in magnitude to previously reported polyoxometalates.[26,27] Synthesis strategy I produced a mixture of uncapped β-$NaSn_{12}$ and γ-$NaSn_{12}$ clusters, as shown in Figure 3.[9] The calculated relative instability of the uncapped α-$NaSn_{12}$ compared to the uncapped β-$NaSn_{12}$ and γ-$NaSn_{12}$ is in accordance with our experimental results, such that it has not been experimentally observed.[9] We hypothesize that the reason γ-$NaSn_{12}$ is 10 kcal mol^{-1} more unstable than β-$NaSn_{12}$ is due to the electrostatic repulsion from the Sn-Sn edge-sharing distance being 3.26 Å, while the Sn-Sn corner-sharing distance is ~3.4-3.5 Å.[9]

Synthesis strategy II performed by Saha *et al.* in 2017 produced a charge neutral single-capped β-$NaSn_{13}$.[5] However, authors found impurities of uncapped $NaSn_{12}$ and Sn_{12} (i.e. the 'football' cluster $[(RSn)_{12}O_{14}(OH)_6]^{2+}$, R=alkyl) co-crystallized with β-$NaSn_{13}$ in unknown quantities, as determined with ESI-MS and ^{119}Sn-NMR. Results for this situation are shown in Figure 3. The computational results performed in this study indicate that single-capped β-$NaSn_{13}$ is more unstable than uncapped β-$NaSn_{12}$ by 37.5 kcal mol^{-1} and uncapped γ-$NaSn_{12}$ by 27.5 kcal mol^{-1}. One interpretation of these results is that a hydrolysis Gibbs free energy difference of 37.5 kcal mol^{-1} between a capped and uncapped system is not sufficient to prevent the respective uncapped system from forming. We also note that it is possible that specific isomers explicitly interact more strongly with the solution, which would not be captured in our mean-field solvation approach.

Synthesis strategy III produced single-capped γ-$NaSn_{13}$ with the presence of uncapped β-$NaSn_{12}$.[9] This result is indicated in Figure 3; the isomers that are circled in bold are the isomers that were observed with this synthesis strategy. The computational results indicate that single-capped γ-$NaSn_{13}$ is more unstable than uncapped β-$NaSn_{12}$ by 33.8 kcal mol^{-1}

and uncapped γ-$NaSn_{12}$ by 23.8 kcal mol^{-1}. The cap on γ-$NaSn_{13}$ yields a short Sn-Sn distance of 3.15 Å between the cap and the nearest tin, which might destabilize the single-capped γ-$NaSn_{13}$ by repulsion, compared to the uncapped γ-$NaSn_{12}$.[9] However, the uncapped γ-$NaSn_{12}$ is not observed. One analysis of these values is that a ΔG_{aq} of 23.8 kcal mol^{-1} between a capped and uncapped system is in fact sufficient to prevent the respective uncapped system from forming.

Synthesis strategy IV performed by Zhu *et al.* in 2019 produced double-capped γ-$NaSn_{14}$.[10] Authors were able to use borate ligands to stabilize the two capping butyltin, which in turn prevented isomerization in solution.[10] It is possible that a more symmetric structure with two caps rather than one allows for a more thermodynamically stable state. The computational results performed in this study indicate that double-capped γ-$NaSn_{14}$ is more stable than uncapped β-$NaSn_{12}$ by 55.1 kcal mol^{-1} and uncapped γ-$NaSn_{12}$ by 65.1 kcal mol^{-1}, as is shown in Figure 3. It seems that since this double-capped γ-$NaSn_{14}$ is more stable than its uncapped counterpart, it dominates in solution. Also, it is possible that since double-capped γ-$NaSn_{14}$ is 55.1 kcal mol^{-1} more stable than β-$NaSn_{12}$, it prevents uncapped-β from forming.

More structures in the Keggin cluster chemical space of Na-Sn need to be synthesized and computationally modeled to truly determine the influence of capping on the thermodynamic stability landscape. What is the energy difference that defines the transition point between forming a mixture of uncapped and capped Keggin clusters, and forming a pure phase? For example, in synthesis strategy III, could uncapped β-$NaSn_{12}$ have been prevented from forming if single-capped γ-$NaSn_{13}$ had only been 23.8 kcal mol^{-1} less stable? Computational tools can be employed to tune the structure of single-capped γ-$NaSn_{13}$ slightly to see if there is room for improvement. If a variation of the single-capped γ-$NaSn_{13}$ is determined, new syntheses can be designed to create this system. This would remove the need to double-cap the structure, and thus maintain simplicity of the structure and a promising photoresist material for EUV lithography. It should be noted that these energy differences are specific to the level of theory, including the implicit solvation, employed in the computational investigation.

5. CONCLUSIONS

The understanding of the fundamental lithographic mechanisms at play during exposure of a Na-Sn Keggin photoresist, can be improved first by exploring the tunability of this Na-Sn Keggin system. Computational results provided vital insight towards understanding the nature of this unique system that favors the lower symmetry Keggin isomers, β and γ. The successful collaborative accumulation of computational and experimental results confirmed that the Sn-Keggin clusters represent the only Keggin ion family to this date that favors these lower symmetry isomers. To prevent a mixture of isomers, strategic capping proved to be successful when the hydrolysis Gibbs free energy differences were large enough. Future work will focus on further probing this Sn-Keggin system's possible capping combinations and changing the central heteroatom.

ACKNOWLEDGEMENTS

The authors gratefully acknowledge the support of the National Science Foundation, Center for Chemical Innovation, grant CHE-1606982.

REFERENCES

[1] "Euv Lithography Finally Ready For Chip Manufacturing - IEEE Spectrum.", <https://spectrum.ieee.org/semiconductors/nanotechnology/euv-lithography-finally-ready-for-chip-manufacturing> (10 September 2019).

[2] Frederick, R. T., Diulus, J. T., Hutchison, D. C., Olsen, M. R., Lyubinetsky, I., Nyman, M.., Herman, G. S., "Surface characterization of tin-based inorganic EUV resists," Advances in Patterning Materials and Processes XXXV, C. K. Hohle and R. Gronheid, Eds., 6, SPIE (2018).

[3] Passarelli, J., Murphy, M., Del Re, R., Sortland, M., Dousharm, L., Vockenhuber, M., Ekinci, Y., Neisser, M., Freedman, D. A., et al., "High-sensitivity molecular organometallic resist for EUV (MORE)," Advances in Patterning Materials and Processes XXXII **9425**, T. I. Wallow and C. K. Hohle, Eds., 94250T, SPIE (2015).

[4] Cardineau, B., Del Re, R., Al-Mashat, H., Marnell, M., Vockenhuber, M., Ekinci, Y., Sarma, C., Neisser, M., Freedman, D. A., et al., "EUV resists based on tin-oxo clusters," Advances in Patterning Materials and Processes XXXI **9051**, T. I. Wallow and C. K. Hohle, Eds., 90511B, SPIE (2014).

[5] Saha, S., Park, D.-H., Hutchison, D. C., Olsen, M. R., Zakharov, L. N., Marsh, D., Goberna-Ferrón, S., Frederick, R. T., Diulus, J. T., et al., "Alkyltin keggin clusters templated by sodium.," Angew. Chem. Int. Ed. Engl. **56**(34), 10140–10144 (2017).

[6] Li, M., Manichev, V., Garfunkel, E. L., Gustafsson, T., Nyman, M., Hutchison, D., Feldman, L. C.., Yu, F., "Novel Sn-based photoresist for high aspect ratio patterning," Advances in Patterning Materials and Processes XXXV, C. K. Hohle and R. Gronheid, Eds., 19, SPIE (2018).

[7] Closser, K. D., Ogletree, D. F., Naulleau, P.., Prendergast, D., "The importance of inner-shell electronic structure for enhancing the EUV absorption of photoresist materials.," J. Chem. Phys. **146**(16), 164106 (2017).

[8] Sharps, M. C., Frederick, R. T., Javitz, M. L., Herman, G. S., Johnson, D. W.., Hutchison, J. E., "Organotin Carboxylate Reagents for Nanopatterning: Chemical Transformations during Direct-Write Electron Beam Processes," Chem. Mater. (2019).

[9] Hutchison, D. C., Stern, R. D., Olsen, M. R., Zakharov, L. N., Persson, K. A.., Nyman, M., "Alkyltin clusters: the less symmetric Keggin isomers.," Dalton Trans. **47**(29), 9804–9813 (2018).

[10] Zhu, Y., Olsen, M. R., Nyman, M., Zhang, L.., Zhang, J., "Stabilizing γ-Alkyltin-Oxo Keggin Ions by Borate Functionalization.," Inorg. Chem. **58**(7), 4534–4539 (2019).

[11] Keggin, J. F., "Structure of the Molecule of 12-Phosphotungstic Acid," Nature **131**(3321), 908–909 (1933).

[12] Zhang, F.-Q., Guan, W., Zhang, Y.-T., Xu, M.-T., Li, J.., Su, Z.-M., "On the origin of the inverted stability order of the reverse-Keggin [(MnO4)(CH3)12Sb12O24]6-: a DFT study of alpha, beta, gamma, delta, and epsilon isomers.," Inorg. Chem. **49**(12), 5472–5481 (2010).

[13] Wills, L. A., Qu, X., Chang, I.-Y., Mustard, T. J. L., Keszler, D. A., Persson, K. A.., Cheong, P. H.-Y., "Group additivity-Pourbaix diagrams advocate thermodynamically stable nanoscale clusters in aqueous environments.," Nat. Commun. **8**, 15852 (2017).

[14] Casasnovas, R., Ortega-Castro, J., Frau, J., Donoso, J.., Muñoz, F., "Theoretical p K_a calculations with continuum model solvents, alternative protocols to thermodynamic cycles," Int. J. Quantum Chem. **114**(20), 1350–1363 (2014).

[15] Sundstrom, E. J., Yang, X., Thoi, V. S., Karunadasa, H. I., Chang, C. J., Long, J. R.., Head-Gordon, M., "Computational and experimental study of the mechanism of hydrogen generation from water by a molecular molybdenum-oxo electrocatalyst.," J. Am. Chem. Soc. **134**(11), 5233–5242 (2012).

[16] Zhang, L., Dembowski, M., Arteaga, A., Hickam, S., Martin, N. P., Zakharov, L. N., Nyman, M.., Burns, P. C., "Energetic trends in monomer building blocks for uranyl peroxide clusters.," Inorg. Chem. **58**(1), 439–445 (2019).

[17] Becke, A. D., "Density-functional thermochemistry. III. The role of exact exchange," J. Chem. Phys. **98**(7), 5648 (1993).

[18] Hariharan, P. C.., Pople, J. A., "The influence of polarization functions on molecular orbital hydrogenation energies," Theor. Chim. Acta **28**(3), 213–222 (1973).

[19] Wadt, W. R.., Hay, P. J., "*Ab initio* effective core potentials for molecular calculations. Potentials for main group elements Na to Bi," J. Chem. Phys. **82**(1), 284–298 (1985).

[20] Marenich, A. V., Cramer, C. J.., Truhlar, D. G., "Universal solvation model based on solute electron density and

on a continuum model of the solvent defined by the bulk dielectric constant and atomic surface tensions.," J. Phys. Chem. B **113**(18), 6378–6396 (2009).
[21] Krishnan, R., Binkley, J. S., Seeger, R.., Pople, J. A., "Self-consistent molecular orbital methods. XX. A basis set for correlated wave functions," J. Chem. Phys. **72**(1), 650 (1980).
[22] López, X., Maestre, J. M., Bo, C.., Poblet, J.-M., "Electronic Properties of Polyoxometalates: A DFT Study of α/β-$[XM_{12}O_{40}]^{n-}$ Relative Stability (M = W, Mo and X a Main Group Element)," J. Am. Chem. Soc. **123**(39), 9571–9576 (2001).
[23] Armstrong, C. R., Casey, W. H.., Navrotsky, A., "Energetics of Al_{13} Keggin cluster compounds.," Proc. Natl. Acad. Sci. USA **108**(36), 14775–14779 (2011).
[24] Wang, W., Fullmer, L. B., Bandeira, N. A. G., Goberna-Ferrón, S., Zakharov, L. N., Bo, C., Keszler, D. A.., Nyman, M., "Crystallizing elusive chromium polycations," Chem **1**(6), 887–901 (2016).
[25] Wang, W., Amiri, M., Kozma, K., Lu, J., Zakharov, L. N.., Nyman, M., "Reaction Pathway to the Only Open-Shell Transition-Metal Keggin Ion without Organic Ligation," Eur J Inorg Chem **2018**(42), 4638–4642 (2018).
[26] López, X.., Poblet, J. M., "DFT study on the five isomers of PW(12)O(40)(3)(-): relative stabilization upon reduction.," Inorg. Chem. **43**(22), 6863–6865 (2004).
[27] López, X., Carbó, J. J., Bo, C.., Poblet, J. M., "Structure, properties and reactivity of polyoxometalates: a theoretical perspective.," Chem. Soc. Rev. **41**(22), 7537–7571 (2012).